J. Physiol. (1981), **315**, *pp.* 569–584
With 9 text-figures
Printed in Great Britain

PROPERTIES AND DISTRIBUTION OF IONIC CONDUCTANCES GENERATING ELECTRORESPONSIVENESS OF MAMMALIAN INFERIOR OLIVARY NEURONES *IN VITRO*

BY RODOLFO LLINÁS AND YOSEF YAROM

From the Department of Physiology and Biophysics, New York University Medical Center, 550 First Avenue, New York, NY 10016, U.S.A.

(*Received 5 September 1980*)

SUMMARY

The electrophysiological properties of the high- and low-threshold Ca spikes described in inferior olivary neurones were analysed in detail.

1. During hyperpolarization the low- and high-threshold Ca action potentials can coexist as two distinct spikes, demonstrating non-mutual exclusion.

2. The high-threshold Ca spike shows a lack of refractoriness, is generated remotely from the site of recording and is composed of several all-or-none components, the last two properties suggesting a dendritic origin.

3. Hyperpolarization of the neurones allows the activation of the low-threshold Ca spike, which has activation properties resembling those of the early *K* conductance described in invertebrates. This low-threshold Ca spike shows refractoriness.

4. The relation between membrane polarization and low-threshold Ca spike is S-shaped. Low-threshold Ca spikes become apparent at −70 mV and have a maximum rate of rise (saturation) at polarization levels more negative than −85 mV. Thus, hyperpolarization removes a voltage-dependent Ca inactivation which is present at normal resting membrane potential (−65 mV).

5. Replacement of extracellular Ca by Ba or addition of tetraethylammonium to the bath corroborates the lack of fast inactivation for the high-threshold Ca spike and the inactivation properties of the low-threshold Ca conductance. It also demonstrates that the duration of the after-depolarization is determined by an interplay between inward Ca current and both voltage-dependent and Ca-dependent K currents.

6. Extracellular recordings from single cells indicate that the Na-dependent spike and the low-threshold Ca action potential are somatic in origin, while the high-threshold Ca spike (after-depolarization) and the hyperpolarization that follows are apparently located in the dendrites.

7. The ionic conductances comprise the main components of the oscillatory behaviour of these cells. The sequence of events leading to oscillation entails initially a low-threshold Ca spike or Na spike, followed by an after-depolarization/after-hyperpolarization sequence and then a post-anodal exaltation produced by a rebound low-threshold Ca spike.

0022-3751/81/5140-1203 $07.50

INTRODUCTION

As shown in the accompanying paper (Llinás & Yarom, 1981) action potentials in inferior olivary (I.O.) neurones are generated by voltage-dependent conductance increases to Na and Ca ions. The Ca-dependent spikes may be subdivided into two distinct types having low and high threshold respectively. The present paper will describe in more detail some properties of the Ca conductances which underlie the two types of Ca spikes.

Basically, three views may be taken with regard to these two varieties of Ca spike. (1) They are generated by a similar Ca conductance (i.e. the same Ca channel) and the differences observed are due only to their differential distribution over the cell membrane. (2) The Ca conductances have a similar distribution but their kinetics are different (i.e. two types of Ca channels). (3) The two conductances, in addition to having different kinetics, are distributed differently. Given the experimental results to be described here, the third possibility seems the most probable.

METHODS

The experimental methods used in this study are identical to those described in the accompanying paper (Llinás & Yarom, 1981). Tetraethylammonium (TEA) was ionophoretically injected intracellularly using a 1M-TEA Cl electrode.

RESULTS

Properties of low- and high-threshold Ca spikes

Coexistence

The coexistence of the two types of Ca spike is of significance because it indicates that they are not mutually exclusive and, thus, represent clearly separable phenomena. The co-activation of the two potentials is illustrated in Fig. 1. Indeed, if an I.O. neurone is activated from a slightly hyperpolarized level (71–75 mV) with square pulses of different amplitudes, one finds (Fig. 1*A*) that a very small stimulus is capable of generating a low-threshold Ca-dependent spike which in turn generates a Na action potential. As the stimulus is increased, the latency for this action potential is shortened. Finally, a larger increase in the stimulus generates a fast-rising Na spike followed by an after-depolarizing potential (ADP) (produced by the low-threshold Ca spike) and, in addition, the high-threshold Ca spike seen as a separate spike (arrow). Normally when these cells are hyperpolarized this high-threshold spike is observed only with large stimuli (3 nA). A similar set of records after the addition of tetrodotoxin (TTX) may be seen in *B*. Note that, as in *A*, these two different Ca spikes can be activated during the same pulses and that when the high-threshold Ca spike is generated, its falling phase is faster than that of the low-threshold spike.

Since these two action potentials can coexist and the high-threshold spike can be evoked when the conductance for the low-threshold Ca spike is inactivated, the possibility that two distinct conductances are actually present was further investigated after the characterization of the Ca spikes themselves.

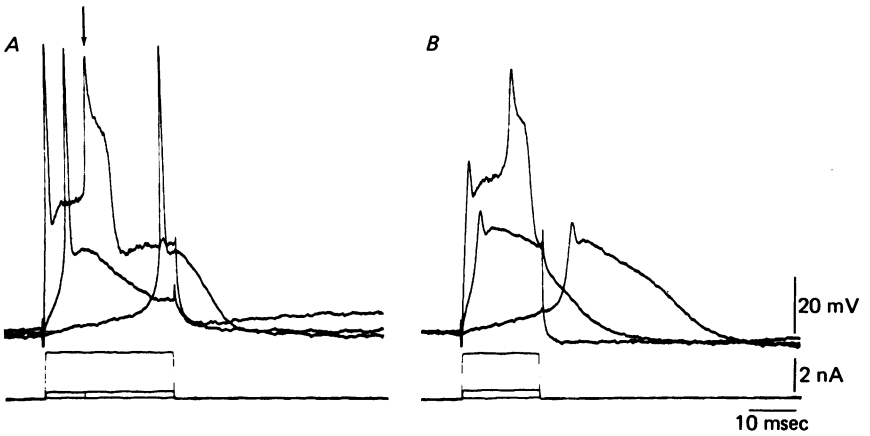

Fig. 1. Co-activation of the two Ca responses. Three superimposed responses to gradually increased current injection. *A*, in a normal solution. *B*, after addition of TTX. Arrow in *A* denotes the high-threshold Ca spike. In both recordings the cell was hyperpolarized by 3 mV.

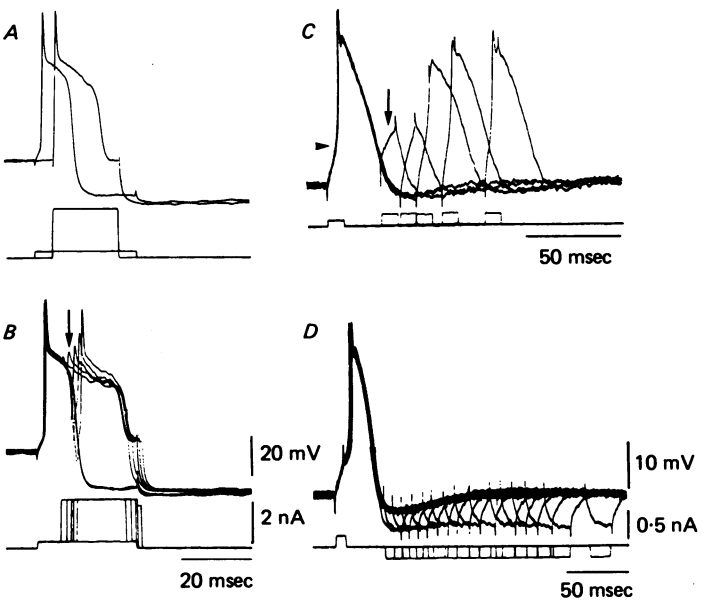

Fig. 2. Test for refractoriness of the high- and low-threshold Ca spikes. *A* and *B*, the absence of refractoriness for the high-threshold Ca spike. *A*, two superimposed responses to different current pulses. Note that the higher stimulus results in a wider ADP. *B*, superimposed traces of five paired stimuli at different intervals show inactivation of Na component (arrow) and summation of the ADPs. *C*, as in *B* showing the refractory period for the low-threshold Ca spike (in the presence of TTX). Arrowhead points to the firing level of the conditioning spike. *D*, conductance increase following the low-threshold Ca spike shown by negative current pulse applied at different intervals after a conditioning spike.

The high-threshold Ca spike

As the high-threshold Ca spike generates a prolonged ADP, a significant question relates to its possible lack of refractoriness. However, the rather fast repolarization which follows this plateau could be taken as a sign of conductance inactivation. In order to study such a possibility, experiments such as those illustrated in Fig. 2 were performed. In *A*, action potentials were generated in an I.O. neurone by two sequential current pulses of different amplitude. The first was produced by a low-amplitude pulse with a duration of approximately 30 msec and the second by a shorter suprathreshold pulse. Other than a difference in the duration of the ADP, these two action potentials were very much alike; i.e. they had the same amplitude for the Na spike and reached the same level of ADP and after-hyperpolarizing potential (AHP). The two stimuli, when given at different intervals, demonstrated a gradual decrease in the amplitude and finally a clear refractory period for the Na spike (arrows in Fig. 2*B*). On the other hand, the addition of the second stimulus actually increased the duration of the ADP from 8 to 22 msec. These results demonstrate the lack of refractoriness for the ADP and indicate that the falling phase of the plateau spike is not due to inactivation of the high-threshold Ca spike. Rather it is probably due to the loss of the equilibrium state between Ca and K conductances which generates such a plateau, as was recently illustrated for the Purkinje cell (Llinás & Sugimori, 1980*a*).

The low-threshold Ca spike

Refractoriness. The low-threshold Ca spike was further studied after the addition of TTX to the bath in order to determine in detail its amplitude and time course. A direct way to determine whether this Ca conductance change inactivates is to test for the presence of a refractory period. As illustrated in Fig. 2*C*, when two direct stimuli were given to a hyperpolarized cell, the second (test) stimulus failed to elicit a spike for intervals less than 50 msec although the test pulse was close to two times threshold for activation of the low-threshold Ca action potential. Indeed, in the first two test stimuli (arrow, Fig. 2*C*) the membrane potential attained amplitudes quite beyond the firing level of the previous spike (arrowhead in Fig. 2*C*).

Since it was deemed possible that a shunt produced by the conditioning spike could reduce the effectiveness of the test stimulus, measurements of conductance change following the conditioning stimulus were obtained. One such experiment is illustrated in *D*. The results indicated that even at the peak of the AHP the input resistance showed a decrease of only 30 % of the resting value, which is not sufficient to explain the absolute refractoriness. Thus, we concluded that the inability of the test pulse to generate a Ca spike at short intervals is due to Ca inactivation. A more detailed description of the de-inactivation properties of this conductance was then attempted.

De-inactivation by membrane hyperpolarization. The voltage dependence of the de-inactivation process was determined in the presence of TTX. The cell was hyperpolarized to different levels and the rate of rise of the Ca-dependent spikes was determined after the de-inactivation process had reached steady state. (The observation of an absolute refractory period for the low-threshold Ca conductance indicates the presence of a time-dependent inactivation. The time dependence of the

de-inactivation by hyperpolarization will not be treated in detail in this paper; however, a steady state is reached within about 50 msec of the onset of the hyperpolarization. At this time depolarizing pulses elicit a constant response.) The results of a set of such experiments are illustrated in Fig. 3. Parts *A–D* illustrate the Ca-dependent responses of a cell to depolarizing current pulses from resting level (*A*) and from successively more negative levels of membrane potential (*B* to *D*). Record *B* was taken at −3 mV from rest (−69 mV) and represents the lowest level of membrane potential at which discernible local responses were obtained. The record

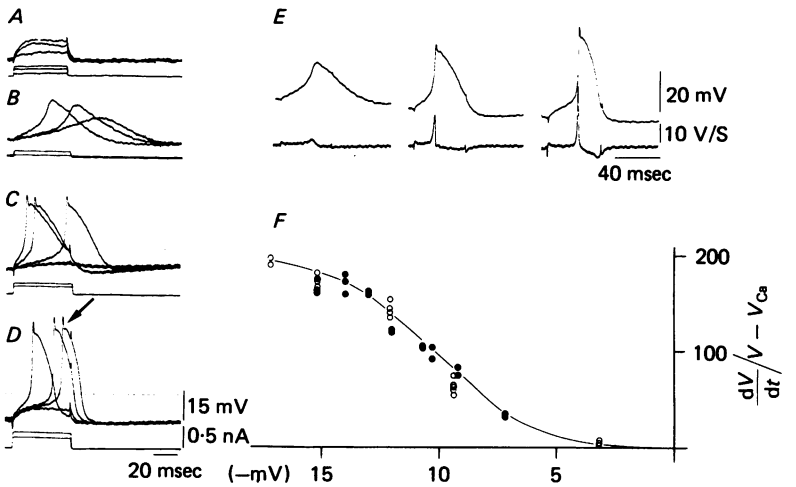

Fig. 3. De-inactivation of the low-threshold Ca spike. *A–D*, membrane response to depolarized current pulses from different level of membrane hyperpolarization in the presence of TTX. Resting level indicated by broken line. Note that the increase in spike amplitude is much larger than expected from a change in driving force. *E*, increase in rise time demonstrated by time derivative of the action potential obtained by means of electrical differentiation with a time constant of 5 μsec. *F*, maximum rate of rise (corrected for driving force) as a function of membrane potential. Open and closed circles represent two different experiments. Abscissa indicates hyperpolarization from resting level; ordinate is the maximum rate of rise divided by driving force.

in *C* was taken at −6 mV and that in *D* at −12 mV, the broken lines in *B* to *D* indicating the resting potential level.

Several features of these action potentials are worth mentioning: they have the same firing level for a given membrane potential, the firing level of the action potential becomes more negative, and its rate of rise steeper as the hyperpolarization increases. Note also that the higher amplitude action potentials have a fast peak followed by a fast initial repolarization (arrow in Fig. 3*D*). This peak, which increases in amplitude with the height of this low-threshold Ca spike is due to the activation of voltage-dependent K conductances as will be demonstrated after TEA injection (see Fig. 5). A rough estimate of the increase in Ca conductance with hyperpolarization was calculated by taking the time derivative of the rising phase of the action potentials as shown in the lower traces in Fig. 3*E*. It was assumed that Ca conductance is proportional to the rate of rise (dV/dt) divided by the Ca driving force

($V_{Ca} - V$), where V is membrane potential and V_{Ca} is equilibrium potential for Ca (taken as +150 mV). A plot of dV/dt corrected for the change in driving force (i.e. $dV/dt(V - V_{Ca})$) as a function of the degree of hyperpolarization after reaching steady state, is shown in *F*. This plot was obtained from measurements made in two representative cells; it is sigmoidal and reaches a plateau near −15 to −20 mV from rest (−80 to −85 mV). The plot indicates that the AHP following a high-threshold action potential is sufficiently large for the de-inactivation of this low-threshold Ca spike and that the active properties of this latter spike are capable of accounting for the rebound depolarization which follows the AHP. The significance of this point will become more apparent when the oscillatory properties of these cells are discussed.

Modification of I.O. electroresponsiveness by Ba and TEA

While the above findings indicate that I.O. neurones display two rather different types of Ca-dependent spikes, the results do not exclude the possibility of a single population of Ca channels having a wide range of voltage sensitivities and rates of inactivation. Two further tests were applied in order to determine more stringently whether the two types of action potential are generated by two truly distinct conductances.

In the first set of experiments, extracellular Ca was replaced by Ba. This ion moves readily through Ca channels (Werman & Grundfest, 1961; Hagiwara, 1973; Hagiwara, Fukuda & Eaton, 1974) and does not activate the Ca-dependent K conductance (Eckert & Lux, 1976). Thus, it is feasible to separate the contribution of a possible Ca inactivation to the falling phase of the spike from a Ca-dependent K conductance. From the results illustrated above, one would expect that in the presence of Ba the high-threshold action potential would be quite prolonged. In addition, given sufficient hyperpolarization and in the presence of TTX, it should be possible to activate the low-threshold Ca spike without activating the high-threshold spike. An example of this type of experiment is shown in Fig. 4. In *A*, direct depolarization of an I.O. cell in the presence of Ba produces a large action potential having a plateau as long as 6 sec (see *B*), confirming the lack of fast inactivation for the Ca conductance which generates the high-threshold spike. In *B* the action potential is shown at a slower sweep speed. Testing of the membrane resistance using short square pulses of current during this spike revealed a large conductance increase during the plateau and a return of the input resistance as the potential approached the resting level (Fig. 4*B*).

The spike shown in Fig. 4*C* was recorded from the same cell as in *A*. In this case the cell was activated from a hyperpolarized membrane level (resting membrane potential given by continuous line) and shows, in contrast to the prolonged spike seen in *A* and *B*, a short-lasting Ba-dependent spike with a fast falling phase. Note that although the current pulse generated a membrane depolarization beyond the firing level of the initial spike, only one action potential was generated. Note also that the membrane potential does not return to the original level at the end of the current pulse, indicating the presence of a Ba local response, possibly of dendritic origin. In *D* a similar response at slower sweep speed shows that with reduced hyperpolarization the early spike is followed by the prolonged high-threshold Ca response. Note again the large conductance change observed during the plateau. These results demonstrate two types of Ba-dependent spikes. If the cell is at rest, direct stimulation elicits a

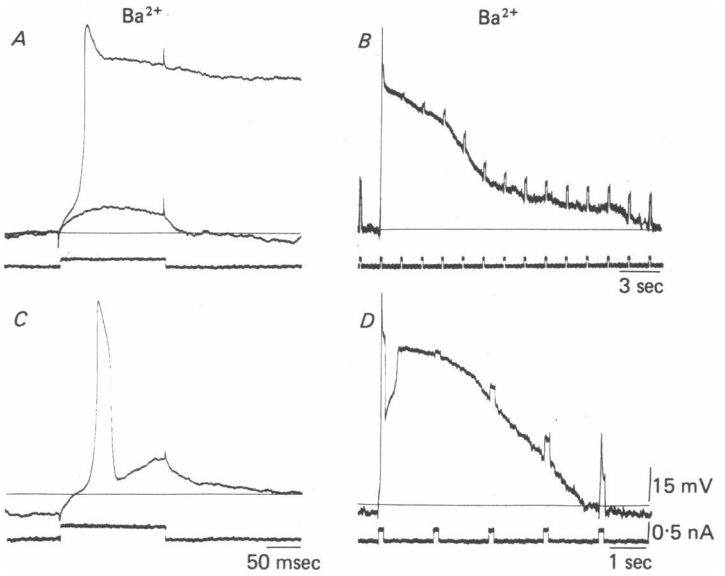

Fig. 4. Ba action potentials. *A* and *B*, depolarizing response generated in cells after replacement of Ca by 2 mM-Ba in the presence of TTX. Note the reduction in input resistance during the spike plateau and the gradual recovery during the repolarization. *C*, short-lasting action potential evoked from 8 mV hyperpolarization. The response is followed by a prolonged depolarization of probable remote origin. *D*, at 3 mV hyperpolarization both types of response may be generated.

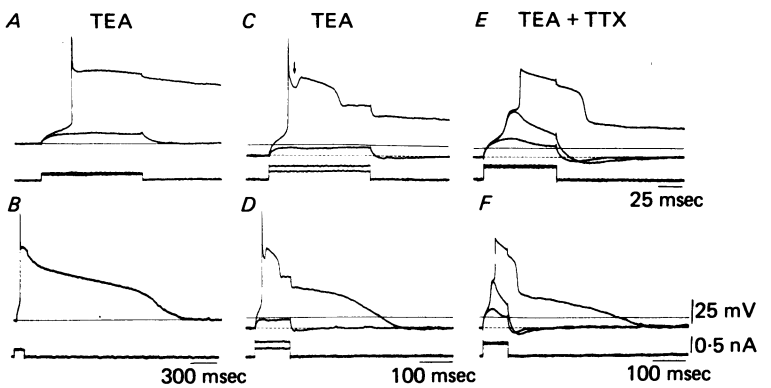

Fig. 5. Electroresponsiveness of I.O. neurone following intracellular injection of TEA. *A* and *B*, prolonged spike elicited by direct stimulation after TEA injection. *C* and *D*, 10 mV hyperpolarization revealed two distinct peaks (indicated by arrow in *C*). Note that the prolonged spike is composed of two plateau levels. *E* and *F*, addition of TTX uncovers two types of Ca spikes: the low-threshold which inactivates and the high-threshold which generates a prolonged depolarization.

prolonged conductance which shows little inactivation (Fig. 4*A*, *B*). On the other hand, if the cell is hyperpolarized, a low-threshold conductance with a fast onset and decay is elicited (Fig. 4*C*).

In a second set of experiments, designed to distinguish further between the two Ca conductances, intracellular injection of TEA was used to reduce the voltage-dependent K conductance (Armstrong & Binstock, 1965). As seen in Fig. 5*A* and *B*, prolonged action potentials are generated following TEA injection. This is especially evident in *B*, where the action potential is shown at a slower sweep speed. Fig. 5*C* and *D* illustrate a similar set of records taken from a slightly hyperpolarized membrane potential level (resting level is given by continuous lines). In these cases two distinct peaks may be observed. The first part of the spike, generated by a Na and low-threshold Ca spike, is followed after a pause (arrow) by the high-threshold Ca action potential. This is seen with particular clarity in Fig. 5 *D*. The high-threshold Ca spike in this case is composed of two phases (Fig. 5*C–F*). The first has a high amplitude and terminates in fast repolarization, followed by a second phase which has a lower amplitude, longer duration and a slow rate of repolarization. Since the high-threshold Ca spike is composed of several all-or-none components (Llinás & Yarom, 1981), the later phase may be generated at a remote site. Such a response would have a lower amplitude due to electrical distance and a longer duration and slower rate of repolarization as it is less affected by somatic hyperpolarization.

Blockage of the Na conductance with TTX after TEA injection (Fig. 5*E* and *F*) demonstrates once again that these two Ca conductances are distinct. Direct stimulation was applied from a hyperpolarized level. The first stimulus was sub-threshold while the slightly higher second stimulus generated a low-threshold Ca-dependent spike (Fig. 5*E*). The third stimulus activated, in addition, the high-threshold Ca action potential. This is shown at a slower sweep speed in *F*. Note the rounded peak for the low-threshold spike, indicating that the fast peak seen in previous records was indeed due to a voltage-dependent K conductance.

Spatial location of low- and high-threshold Ca-dependent spikes

While the results so far presented suggest that two types of Ca conductance underlie the two Ca spikes, information regarding the actual distribution of these conductances is difficult to obtain from such evidence. In principle, these two sets of Ca channels could be present at the same location, the difference in threshold relating more to their activation kinetics than to their spatial distribution. In order to gain further insight into this problem, extracellular recordings were obtained from the I.O. cells following antidromic invasion.

Of significance here was the finding that the time course and overall shape of the unitary extracellular spikes could be modified in a predictable manner by extracelluar current injection via the recording micro-electrode. A correlation between the unitary field potential and the intracellular recordings was attempted by recording the extracellular fields and comparing them with the potentials obtained from the same cell following impalement. Sets of intra- and extracellular pairs are illustrated in Fig. 6. In *A*, the extracellular potential (lower record) was obtained in the absence of polarization. The antidromic spike was characterized by a positive–negative wave followed by a slowly rising positivity having several wavelets. The waveform of this extracellular spike is in keeping with that of the intracellular action potential

obtained in the same cell following penetration (upper trace). The behaviour of the intra- and extracellularly recorded potentials is illustrated in Fig. 6*B*, *C* and *D*. The changes in the spike waveform during extracellular anodal polarization are comparable to the changes observed intracellularly by direct hyperpolarization of the cell. A 20 nA positive current injected extracellularly produced a simplified extracellular action

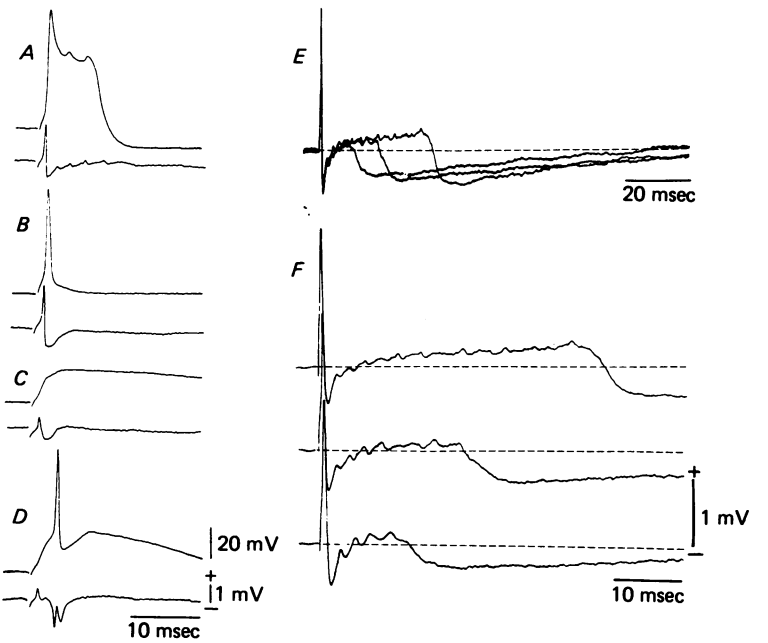

Fig. 6. The effect of membrane potential on intra- and extracellular recordings. *A–D*, intracellular recording of an antidromically evoked action potential at different membrane potentials (upper traces), and similar antidromic response recorded outside the cell during extracellular d.c. anodic polarization (lower traces). *A*, resting level; *B–D*, 5, 8 and 15 mV hyperpolarization respectively. *E* and *F*, extracellular recording of an antidromic response during three different levels of cathodic polarization. In *E* the three responses are superimposed in order to demonstrate increased duration for the positivity and late negativity which corresponds to the ADP and AHP intracellularly. *F*, the same responses as in *E* but displayed separately and at faster sweep speed.

potential which becomes positive–negative (*B*) without the after-positivity seen in *A*. Intracellularly, hyperpolarization by 5 mV produced a total disappearance of the ADP, indicating that the ADP seen intracellularly can be correlated with the extracellular slow positive field. Increased anodal polarization reduced the extracellularly recorded spike to a short positivity followed by a clear negative wave (*C*). Intracellularly, with increased hyperpolarization the Na-dependent spike was blocked but a prolonged depolarization corresponding to the extracellular negativity could be seen. A final increase in anodal polarization produced extracellularly the appearance of a fast negative–positive action potential riding on a large negative wave (*D*). Intracellularly, increased hyperpolarization further de-inactivated the Ca conductance and increased the amplitude of the low-threshold Ca spike enough to activate a Na action potential (*D*).

In the same cell, extracellular cathodal polarization generated, following the initial

positive–negative spike (*E*), a positive-going after-potential which abruptly changed to a prolonged negativity after different plateau durations (*F*). Intracellularly, d.c. depolarization was shown to increase the duration of the ADP (Llinás & Yarom, 1981, Fig. 2*B*).

Oscillatory properties of I.O. *neurones*

In experiments *in vivo*, I.O. neurones are known to oscillate at a frequency of 5–10/sec with great regularity (Armstrong, Eccles, Harvey & Matthews, 1968; Crill, 1970; Llinás & Volkind, 1973; Llinás, Baker & Sotelo, 1974; Headley & Lodge, 1976). It would be expected that interplay between the conductances described here and in

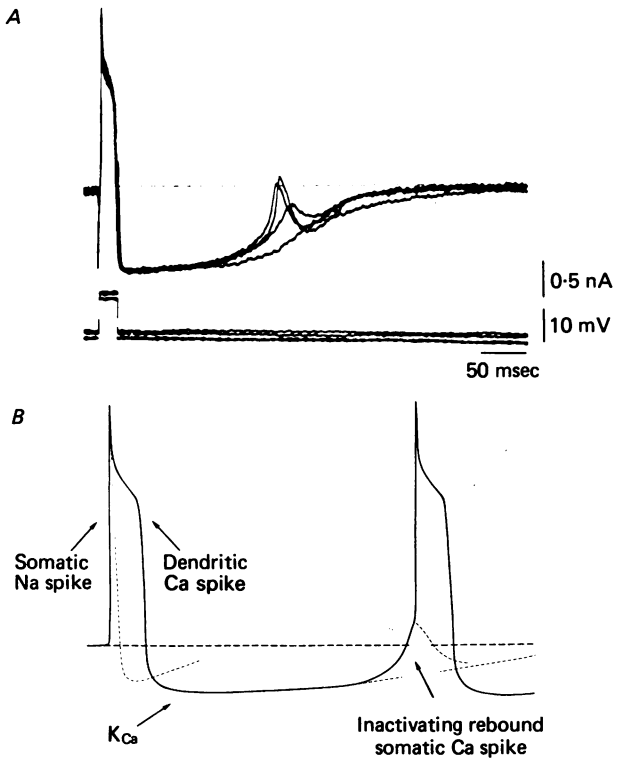

Fig. 7. Oscillatory behaviour of I.O. neurones in the presence of TTX. *A*, direct activation of an action potential recorded at slightly depolarized membrane, demonstrating an active rebound excitation. *B*, schematic representation of the oscillatory behaviour. A somatic Na spike triggers dendritic Ca response (high-threshold Ca spike) which activates a Ca-dependent K current, which in turn de-inactivates the somatic Ca spike.

the accompanying paper (Llinás & Yarom, 1981) should be capable of generating many aspects of the I.O. oscillatory behaviour. It should be possible to trigger the mechanism by either antidromic or orthodromic activation which would generate a dendritic ADP–AHP sequence. As illustrated in this and the accompanying paper, the AHP is usually followed by a rebound somatic Ca spike often large enough to generate a secondary Na spike which in turn initiates the whole process once again (Fig. 7*B*). Such phenomena actually occur frequently in these neurones, especially if

they are slightly hyperpolarized (more than 70 mV resting potential). An example of such an oscillatory property (Fig. 7*A*) is indeed characterized by a very rapid rebound Ca activation. Because in this experiment Na conductance was blocked with TTX, no secondary Na action potential was seen.

Oscillatory Ca spikes occur at two frequencies, each generated by a separate mechanism. If the cell (especially the dendrites) is partly depolarized by background activity, activation of the Na spike can successfully generate the firing of the dendrites which, as described above, produce a rebound somatic Ca spike. On other occasions, due to a more negative membrane potential, the Na spike does not activate a dendritic potential but may be capable of producing a certain amount of sequential Ca–K activation in the soma which in turn triggers the somatic rebound. In these cases, firing frequencies may be as high as 15/sec, rather than the usual 5–8/sec. The modulation of membrane potential level and of dendritic excitability seems to be a crucial parameter in determining the frequency of oscillation in these neurones.

DISCUSSION

This paper is concerned with the different properties of high- and low-threshold, voltage-dependent Ca conductances and their distribution in the cell membrane. The results indicate that the low-threshold Ca conductance is most prominent at the soma while the high-threshold Ca conductance is very likely restricted to the dendritic processes. Besides their spatial separation, these two conductances seem to have other fundamental differences relating to voltage-dependent inactivation.

High-threshold Ca spikes: a non-inactivating dendritic Ca conductance

The evidence for a dendritic location of the non-inactivating Ca conductance rests on two points: (1) the high threshold for Ca-dependent spikes to somatic current injection, and (2) the extracellular positivity that such spikes generate. The evidence for non-inactivation consists of: (1) the absence of a refractory period, and (2) the ability to generate prolonged spikes following addition of Ba to the bath or intracellular injection of TEA.

Non-inactivating properties. Although the absence of a voltage-dependent inactivation is implied in the lack of a refractory period, the limited duration of the dendritic Ca spikes (10–30 msec) could indicate inactivation. However, the relatively short duration of the dendritic spike is due to the activation of voltage- and Ca-dependent K currents which hyperpolarize the cell and decrease its resistance, preventing the Ca conductance from maintaining its regenerative property. Thus, following the addition of Ba to the extracellular medium, prolonged action potentials lasting for up to 6 sec were observed (Fig. 4*B*). During this period there was a continuous reduction in the amplitude of the Ba spike, probably due to slow inactivation (Rudy, 1978). However, because this process is very slow compared with the time course of the Na conductances, the term 'non-inactivating' is used.

Dendritic location. While the distribution of extracellular currents is quite clear for the Na-dependent portion of the I.O. action potential, the main question here concerns the site of origin of the ADP. An interpretation of the spatial distribution of ionic conductances generating these different action potentials is illustrated in Fig. 8; the

three components of the antidromic I.O. action potential recorded intracellularly (first column), from resting membrane level, and extracellularly (second column) are shown. In *A* the Na component of the action potential is seen intracellularly as a sharp positivity and extracellularly as a positive–negative wave. The interpretation of this field is straightforward, as shown in the diagram to the right. As expected from a closed field in a volume conductor (Lorente de Nó, 1947), the incoming antidromic action potential generates a somatic current source and then a sink as the action potential reaches the somatic region (cf. Hubbard, Llinás, & Quastel, 1969). This somatic current sink is indicated in the diagram to the right by arrows showing current flow from dendrites into the somatic region.

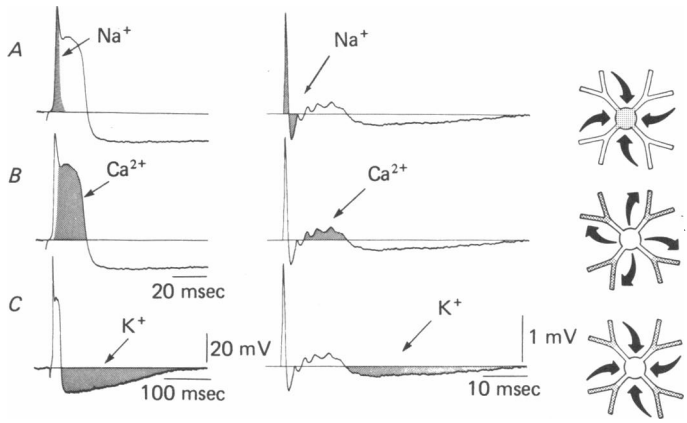

Fig. 8. Schematic description of the extracellular current flow for high-threshold Ca spike. First column: intracellular recording of antidromically evoked action potential. Second column: corresponding response recorded extracellularly. Third column: schematic representation of the current flow for the different components of the action potential. *A*, Na-dependent current. *B*, high-threshold Ca current. *C*, Ca- and voltage-dependent K current. Note the different time scale. For details, see text.

The second part of the action potential is the high-threshold Ca-dependent spike. If the Ca conductance generating this spike were to be located at the soma, a negativity (as with the Na-dependent component) should be observed. However, a positivity was recorded at that time (see also Fig. 6*E* and *F*). This implies then, as illustrated in the diagram to the right in Fig. 8, that the Ca conductance must have occurred remotely as the soma served as a current source for the Ca sink which must have occurred in the dendrites. This is illustrated in the diagram by arrows indicating current flow from the soma into the dendrites. Since the field potential which corresponded to the AHP (*C*) was negative (i.e. the soma served as a current sink), the active current source produced by the K conductance must also be located at the dendritic level. This is illustrated in the diagram to the right of *C*. The high threshold of this potential further reinforced the conclusion regarding the dendritic origin of this spike and is in accordance with similar findings in Purkinje cells (Llinás & Sugimori, 1980*b*) and in hippocampal neurones (Wong, Prince & Basbaum, 1979).

Low-threshold Ca spikes: an inactivating somatic Ca conductance

Inactivating properties. As opposed to the dendritic Ca conductance which is always obtained in I.O. neurones upon depolarization, the low-threshold Ca conductance change can only be seen following I.O. hyperpolarization, as the conductance which generates this spike is inactivated at resting potential (−65 mV). This de-inactivation is not only voltage-dependent but has a time dependence as well (Llinás & Yarom, 1980).

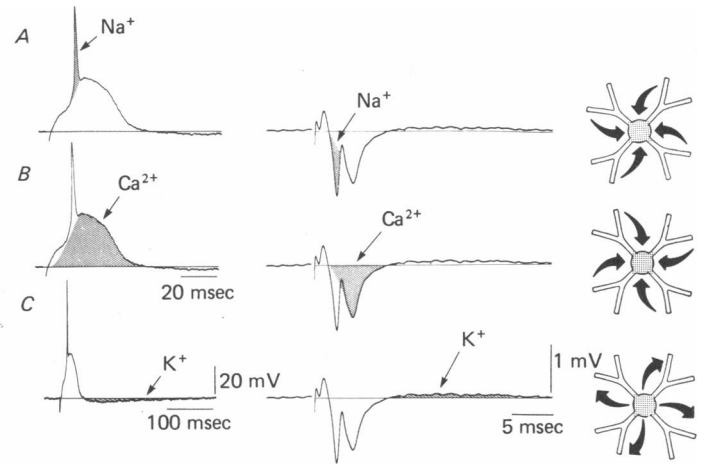

Fig. 9. Schematic description of extracellular current flow for low-threshold Ca spike. First column: intracellular recording of an antidromically evoked response during 10 mV hyperpolarization. Second column: an antidromic response recorded extracellularly during positive d.c. injection (20 nA). Third column: schematic representation of the current flow for the different components of the Ca action potential. *A*, Na current. *B*, low-threshold Ca current. *C*, voltage- and/or Ca-dependent K current. Note the different time scale. For details, see text.

Direct evidence for the inactivation of this conductance was obtained following intracellular injection of TEA or extracellular Ba. The finding that the somatic Ca action potential has a sharp falling phase after 10 msec, even with reduced K conductance or Ca-dependent K conductance (under which conditions the Ca dendritic spike may last for many seconds), is taken as demonstrative of a true voltage-dependent inactivation. Furthermore, analysis of the rate of rise of somatic Ca action potentials as a function of membrane hyperpolarization indicates that maximum de-inactivation is obtained at 15–20 mV from rest (−90 to −95 mV) (Fig. 3).

Somatic location. The extracellular field potentials corresponding to the low-threshold Ca spike illustrated in Fig. 6*D* are seen in Fig. 9. Here intracellular recordings are shown to the left and the extracellular potentials to the right. On the extreme right are diagrams indicating the direction of current flow during the different components of these action potentials. In *A* the Na action potential is seen to be generated from the rising phase of the low-threshold Ca-dependent action potential. As is to be expected, this Na spike generates a clear extracellular negativity indicating, as shown

to the right, a somatic current sink. In *B* the low-threshold Ca spike is seen to generate an extracellular negative field in contrast to the positivity produced by the high-threshold Ca spike. This large negativity shows that this Ca spike was elicited at somatic level. Furthermore, because the antidromic invasion activates the low-threshold Ca conductance at a lower threshold than the Na spike, when the cell is hyperpolarized the low-threshold Ca conductance must dominate somatic excitability. In *C* the AHP which follows the low-threshold Ca spike is shown at a lower sweep speed. The extracellular potential evoked at this time was positive; accordingly, we conclude that the hyperpolarization must have been produced by a K conductance change located at the somatic level.

Relation between electrical activity of I.O. *neurones seen* in vitro *and that observed* in vivo

While the results described in this paper represent electrophysiological details regarding a mammalian neurone *in vitro*, the question may be posed as to how these results relate to the activity observed *in vivo* at the unitary level or at the level of the olivo-cerebellar system as a whole.

Extracellular spikes. The extracellular unitary potentials recorded *in vivo* often resemble those described *in vitro* as due to the somatic Ca spike, i.e. mainly two short negative waves (Fig. 6*D*) (Armstrong & Harvey, 1966; Armstrong *et al.* 1968; Duggan, Lodge, Headley & Biscoe, 1973; Headley & Lodge, 1976). On other occasions they resemble the negative–positive–negative wave produced by the full activation of the dendritic tree (Armstrong *et al.* 1968; Crill, 1970). These variations reflect, most probably, the resting potentials of the cells under study. Indeed levels of anaesthesia may be of importance in these variations. However, the point of interest here relates to the fact that the two types of extracellular spikes may be observed both *in vivo* and *in vitro*.

Low frequency of response. A second prevalent finding regarding I.O. activity and/or climbing fibre activation of Purkinje cells is its rather low firing rate (e.g. Armstrong & Harvey, 1966; Simpson & Alley, 1974; Armstrong & Rawson, 1979). The long duration of the AHP seen here is most probably the origin of this very characteristic low firing rate of I.O. cells. The same mechanism would also explain the poor ability of these cells to follow high-frequency stimulation.

Repetitive axonal firing. At the Purkinje cell level, climbing fibre activation following direct stimulation of the white matter is characterized by a single excitatory post-synaptic potential (e.p.s.p.), often followed by an I.O. reflex (Eccles, Llinás & Sasaki, 1966). The I.O. reflex is composed of a train of climbing fibre e.p.s.p.s having a frequency of approximately 400–500/sec and consisting of one to four e,p.s.p.s, produced by repetitive firing of the I.O. axon. The origin of such repetitive firing is most probably related to the wavelets which rise on the ADP and which are blocked by TTX, indicating firing at the axonic level. Regarding the I.O. reflex itself, the almost invariant latency denotes, as proposed before, that it is due to electrotonic coupling between I.O. cells (Llinás *et al.* 1974; Llinás & Yarom, 1981).

Oscillation. Finally, the action of harmaline in the I.O. has been a puzzling phenomenon, as the presence of this drug produced a protracted I.O. oscillation of remarkably constant frequency (see de Montigny & Lamarre, 1973; Llinás & Volkind,

1973). As recently described, harmaline causes a hyperpolarization of the I.O. neurone (Llinás & Yarom, 1980). Furthermore, this hyperpolarization de-inactivates the somatic Ca conductance thus enabling the mechanism for oscillatory behaviour described here. The possibility that this type of rebound Ca current may not be exclusive to the I.O. then becomes a point of general interest. Indeed, such a mechanism may be found in other oscillatory systems in the mammalian central nervous system. In particular, in the thalamus, which occupies a similar central way-station for cerebral cortical afferents as does the I.O. for cerebellar cortical afferents, such a mechanism could underlie generation of the alpha rhythm.

Research was supported by United States Public Health Service program grant NS-13742 from the National Institute of Neurological and Communicative Disorders and Stroke.

REFERENCES

ARMSTRONG, C. M. & BINSTOCK, L. (1965). Anomalous rectification in the squid giant axon injected with tetraethylammonium chloride. *J. gen. Physiol.* **48**, 859–872.

ARMSTRONG, D. M., ECCLES, J. C., HARVEY, R. J. & MATTHEWS, P. B. C. (1968). Responses in the dorsal accessory olive of the cat to stimulation of hind limb afferents. *J. Physiol.* **194**, 125–145.

ARMSTRONG, D. M. & HARVEY, R. J. (1966). Responses in the inferior olive to stimulation of the cerebellar and cerebral cortices in the cat. *J. Physiol.* **187**, 553–574.

ARMSTRONG, D. M. & RAWSON, J. A. (1979). Activity patterns of cerebellar cortical neurones and climbing fibre afferents in the awake cat. *J. Physiol.* **289**, 425–448.

CRILL, W. E. (1970). Unitary multiple-spiked responses in cat inferior olive nucleus. *J. Neurophysiol.* **33**, 199–209.

DUGGAN, A. W., LODGE, D., HEADLEY, P. M. & BISCOE, T. J. (1973). Effects of excitants on neurons and cerebellar-evoked field potential in the inferior olivary complex of the rat. *Brain Res.* **64**, 397–401.

ECCLES, J. C., LLINÁS, R. & SASAKI, K. (1966). The excitatory synaptic actions of climbing fibres on the Purkinje cells of the cerebellum. *J. Physiol.* **182**, 268–296.

ECKERT, R. & LUX, H. D. (1976). A voltage-sensitive persistent calcium conductance in neuronal somata of *Helix*. *J. Physiol.* **254**, 129–151.

HAGIWARA, S. (1973). Ca spikes. *Adv. Biophys.* **4**, 71–102.

HAGIWARA, S., FUKUDA, J. & EATON, D. C. (1974). Membrane currents carried by Ca, Sr and Ba in barnacle muscle fiber during voltage clamp. *J. gen. Physiol.* **63**, 564–578.

HEADLEY, P. M. & LODGE, D. (1976). Studies on field potentials and on single cells in the inferior olivary complex of the rat. *Brain Res.* **101**, 445–459.

HUBBARD, J. I., LLINÁS, R. & QUASTEL, D. M. J. (1969). *Electrophysiological analysis of synaptic transmission* (monograph of the Physiological Society). London, Edward Arnold; Baltimore, Williams & Wilkins.

LLINÁS, R., BAKER, R. & SOTELO, C. (1974). Electrotonic coupling between neurones in cat inferior olive. *J. Neurophysiol.* **37**, 560–571.

LLINÁS, R. & SUGIMORI, M. (1980*a*). Electrophysiological properties of *in vitro* Purkinje cell somata in mammalian cerebellar slices. *J. Physiol.* **305**, 171–195.

LLINÁS, R. & SUGIMORI, M. (1980*b*). Electrophysiological properties of *in vitro* Purkinje cell dendrites in mammalian cerebellar slices. *J. Physiol.* **305**, 197–213.

LLINÁS, R. & VOLKIND, R. A. (1973). The olivo-cerebellar system: Functional properties as revealed by harmaline-induced tremor. *Exp. Brain Res.* **18**, 69–87.

LLINÁS, R. & YAROM, Y. (1980). Electrophysiological properties of mammalian inferior olivary cells *in vitro*. In *The inferior olivary nucleus: Anatomy and Physiology*, ed. COURVILLE, J., DE MONTIGNY, C. & LAMARRE, Y., pp. 379–388. New York: Raven Press.

LLINÁS, R. & YAROM, Y. (1981). Electrophysiology of mammalian inferior olivary neurons *in vitro*: different types of voltage-dependent ionic conductances. *J. Physiol.* **315**, 549–567.

LORENTE DE NÓ, R. (1947). Action potential of the motoneurons of the hypoglossus nucleus. *J. cell comp. Physiol.* **29**, 207–288.

MONTIGNY, C. DE & LAMARRE, Y. (1973). Rhythmic activity induced by harmaline in the olivo-cerebellar–bulbar system of the cat. *Brain Res.* **53**, 81–95.

RUDY, B. (1978). Slow inactivation of the sodium conductance in squid giant axons. Pronase resistance. *J. Physiol.* **283**, 1–21.

SIMPSON, J. I. & ALLEY, K. E. (1974). Visual climbing fiber input to rabbit vestibulo-cerebellum: a source of direction-specific information. *Brain Res.* **82**, 302–308.

WERMAN, R. & GRUNDFEST, H. (1961). Graded and all-or-none electrogenesis in arthropod muscle. II. The effects of alkali-earth and onium ions on lobster muscle fibres. *J. gen. Physiol.* **44**, 997–1027.

WONG, R. K. S., PRINCE, D. A. & BASBAUM, A. I. (1979). Intradendritic recordings from hippocampal neurons. *Proc. natn. Acad. Sci. U.S.A.* **76**, 986–990.